

# Augmented Reality Assisted Surgical Navigation System for Epidural Needle Intervention\*

Sunghwan Lim<sup>1</sup>, Junhyoung Ha<sup>1</sup>, Seongmin Yoon<sup>1</sup>, Young Tae Sohn<sup>2</sup>,  
Joonho Seo<sup>3</sup>, Jae Chul Koh<sup>4†</sup>, and Deukhee Lee<sup>1†</sup>

**Abstract**—An augmented reality (AR)-assisted surgical navigation system was developed for epidural needle intervention. The system includes three components: a virtual reality-based surgical planning software, a patient and tool tracking system, and an AR-based surgical navigation system. A three-dimensional (3D) path plan for the epidural needle was established on the preoperative computed tomography (CT) image. The plan is then registered to the intraoperative space by 3D models of the target vertebrae using skin markers and real-time tracking information. In the procedure, the plan and tracking information are transmitted to the head-mounted display (HMD) through a wireless network such that the device directly visualizes the plan onto the back surface of the patient. The physician determines the entry point and inserts the needle into the target based on the direct visual guidance of the system. An experiment was conducted to validate the system using two torso phantoms that mimic human respiration. The experimental results demonstrated that the time and the number of X-rays required for needle insertion were significantly decreased by the proposed method ( $43.6 \pm 20.55\text{sec}$ ,  $2.9 \pm 1.3\text{times}$ ) compared to those of the conventional fluoroscopy-guided approach ( $124.5 \pm 46.7\text{s}$ ,  $9.3 \pm 2.4\text{times}$ ), whereas the average targeting errors were similar in both cases. The proposed system may potentially decrease ionizing radiation exposure not only to the patient but also to the medical team.

**Clinical relevance**— The AR-based navigation system intuitively assists physicians in inserting an epidural needle. It enables safe needle insertion with 69% less radiation exposure compared to the conventional fluoroscopy-guided approach.

## I. INTRODUCTION

Image-guided spine intervention (IGSI) is a primary strategy for managing back pain [1], and its related technologies and market are emerging [2]. In IGSI, introducing needle placement is the most critical step of the procedure. A needle

needs to be inserted into the three-joint complex, which involves pain-sensitive structures including nerve roots, dura, posterior longitudinal ligaments, outer annular fibers of the disk, facet joints, and joint capsules.

Although several systems use various medical imaging techniques, including ultrasound [3] and magnetic resonance [4] images, the mainstream of the IGSI remains under fluoroscopic guidance [5]. In fluoroscopy-guided spine interventions, the patient is placed in a prone position on the fluoroscopy table. The physician inserts a needle into the target, identifying the position of the needle using anteroposterior and lateral views of the lumbar spine using fluoroscopy [5]. This process involves a significant ionizing radiation exposure not only to the patient but also to the medical team.

Several augmented reality (AR)-based navigation techniques have been proposed to reduce radiation exposure during fluoroscopy-guided spine intervention. Elmi-Terander et al. presented an AR-based navigation system that provides AR views, including synthetic X-ray images generated from a cone beam computed tomography (CT) volume and augmented on real-time optical videos [6]. AR views are shown on the monitors. Other studies reported AR-based systems that use head-mounted displays (HMDs) rather than monitors, providing an AR view directly in the physician's field of view [7], [8]. However, these systems did not consider human respiration [7] or relied on manual image-patient registration [7], [8].

We developed an AR-assisted surgical navigation system for epidural needle intervention that enables intuitive and active visual guidance and minimizes radiation exposure to patients and medical teams.

## II. MATERIALS AND METHODS

### A. System Overview

Fig. 1 shows the overview of the AR-assisted surgical navigation system for epidural needle intervention. The system consists of three components: a virtual reality (VR)-based surgical planning system, a patient and tool tracking system, and an AR-based surgical navigation system. Fig. 2 shows the workflow of the system that describes a relationship of these three components. A three-dimensional (3D) path plan of the epidural needle is established using the VR-based planning software under the supervision of the surgeon. The preoperative patient image is then registered to the intraoperative space along with the 3D path plan of the needle. In the intraoperative procedure, the tracking system

\*This study was supported by Ministry of Trade Industry & Energy (MOTIE, Korea), Ministry of Science & ICT (MSIT, Korea), and Ministry of Health & Welfare (MOHW, Korea) under the Technology Development Program for AI-Bio-Robot-Medicine Convergence (20001655).

<sup>†</sup>Jae Chul Koh and Deukhee Lee have contributed equally to the project organization and execution and should be co-last authors.

<sup>1</sup>The authors are with Center for Healthcare Robotics, Artificial Intelligence and Robotics Institute, Korea Institute of Science and Technology, Seoul 02792, Korea (SL: slim@kist.re.kr, DL: dkylee@kist.re.kr)

<sup>2</sup>Young Tae Sohn is with Center for Bionics, Biomedical Research Institute, Korea Institute of Science and Technology, Seoul 02792, Korea ytsohn@kist.re.kr

<sup>3</sup>Joonho Seo is with the Department of Medical Assistant Robot, Korea Institute of Machinery and Materials, Daegu 34103, Korea jhseo@kimm.re.kr

<sup>4</sup>Jae Chul Koh is with the Department of Anesthesiology and Pain Medicine, Korea University Anam Hospital, Seoul 02841, Korea jaykoh@korea.ac.kr



Fig. 1: System overview of the AR-assisted surgical navigation system for epidural needle intervention

traces the movements of the patient and needle in real-time. The tracking information of the patient and needle is then transmitted to the HMD (Hololens2, Microsoft, USA) through the wireless network such that the device directly visualizes the 3D path of the epidural needle onto the back surface of the patient. The surgeon determines the insertion point of the needle and inserts the needle toward the target based on the visual guidance of the system. Further details for each system are contained in the following sections.

### B. VR-based Surgical Planning

VR-based surgical planning software was developed using open-source libraries such as the visualization toolkit [9] and insight toolkit [10], as shown in Fig. 3). The software is capable of rendering CT volume, segmenting vertebrae and a skin surface, and re-slicing a volume image. A safe and feasible path for the epidural needle can be generated using this software. The path of the needle is determined by selecting two points: one point at the target and another point at the back skin surface of the patient. The software also includes a special function to provide a safety color map on the back surface of the patient. The color map shows the closest distances between the virtual needle path and the closest point of the vertebrae of interest in different colors, such that the surgeon could select a safe entry point that avoids collisions with the vertebrae of interest. The blue and red areas in Fig. 3 represent the safe and unsafe regions, respectively. The final safe and feasible path of the

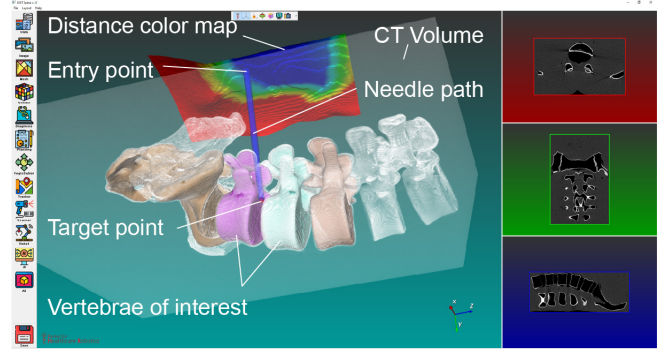


Fig. 3: VR-based needle path planning software showing a CT volume, vertebrae of interest, a needle path connecting entry and target points, and a distance color map

epidural needle is determined under the supervision of the physician considering comprehensive conditions, such as the anatomical structure of the spinal nerve and distance color map on the back surface.

### C. Image-Patient Registration

Special skin markers were developed such that the markers were visible in both the CT images and the patient tracking system. A sheet sprayed with retroreflective paint and thin multiple copper sheets was precisely cut out to have the shape of a circle with a diameter of 10 mm. Multiple copper sheets were then affixed to the retroreflective sheet, as shown in Fig. 4a. These markers are attached to the back surface of the patient and imaged with a CT scan prior to the procedure, whereas the positions of the markers were traced in real-time during the procedure using the patient tracking system. Image-patient registration is performed prior to the procedure using these skin markers. The registration involves a process to find a transformation matrix  $F = [R, \vec{p}]$ ,  $R \in \mathbb{R}^{3 \times 3}$ ,  $\vec{p} \in \mathbb{R}^3$  such that,

$$\vec{t}_i = R\vec{c}_i + \vec{p} \quad (1)$$

where  $\vec{c}_i \in \mathbb{R}^3$  represents the center point of the  $i$ th marker extracted from the CT image before the procedure, whereas  $\vec{t}_i \in \mathbb{R}^3$  represents the center point of the corresponding  $i$ th marker traced by the patient tracking system in real time during the procedure.

The rotational component  $R$  can be found using any of the iterative approaches, the singular value decomposition-based approach [11], or quaternion-based approach [12], [13]. The positional component  $\vec{p}$  is then obtained as follows:

$$\vec{p} = \bar{t} - R\bar{c} \quad (2)$$

where  $\bar{t} = \frac{1}{N} \sum_{i=1}^N \vec{t}_i$ ,  $\bar{c} = \frac{1}{N} \sum_{i=1}^N \vec{c}_i$ , and  $N$  is the number of markers.

### D. Patient and Tool Tracking

A multiple-tracker-based patient and tool-tracking system was developed. The tracking system consists of three optical 3D pose trackers, which were designed and developed by our team (Fig. 4 (b)[14]. The three trackers are distributed and fixed to the ceiling of the operating room such that all the

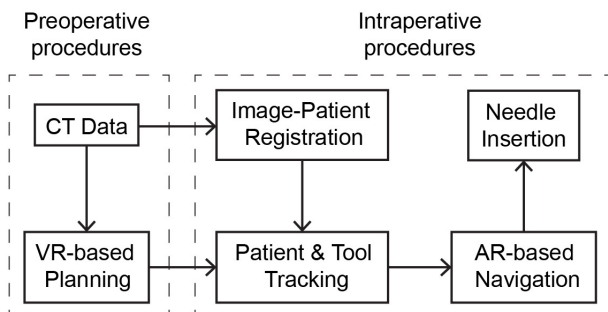


Fig. 2: Workflow of the AR-based surgical navigation system

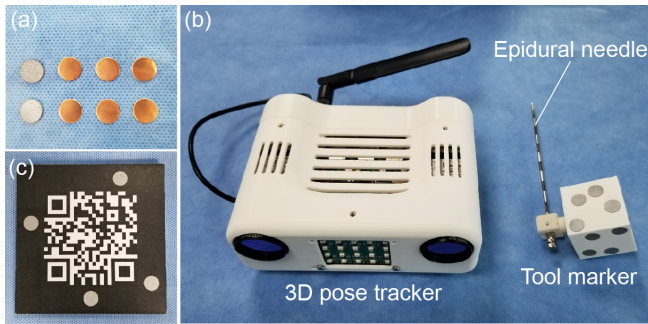


Fig. 4: Patient and tool tracking system: (a) skin markers, (b) 3D pose tracker, epidural needle, tool marker, and (c) reference marker including retroreflective markers and a QR code

trackers align to the surgical field from different directions, as shown in Fig. 1). This configuration of the multiple trackers could allow the tracking system to acquire stable data, even if the markers are occluded by medical devices and tools or medical staff during the procedure.

A reference marker was specially designed and constructed to have four retroreflective markers on the edges and a rectangular quick response (QR) code at the center of the marker such that the 3D pose of the marker can be traced by both the tracking system and the vision sensor of the HMD device, as shown in Fig. 4 (c)]. The QR code also includes patient information, which can be identified using AR-based surgical navigation software. The pose and position data of the tool and skin markers were measured along with the pose of the reference marker, which was fixed to the patient bed with a passive arm and placed near the surgical field, as shown in Fig. 1). The tracking data were then transmitted to the navigation software over the wireless network. The relative poses or positions from the reference marker coordinate system to each tool or skin marker were internally calculated using the navigation software. This enables free movement of the trackers during the procedures, which can occur by chance or on purpose. The relative poses of the tool or skin markers are then selected based on the visibility of the markers from each tracker and averaged to increase the stability of the tracking system.

#### E. AR-based Surgical Navigation

An HMD (HoloLens 2, Microsoft, USA) was used to visualize the 3D model of the spine and the preoperative path plan of the epidural needle onto the back surface of the patient. The 3D pose of the spine model and needle path plan with respect to the reference marker coordinate system was computed with the navigation software by performing image-patient registration for each frame. Thereafter, the relative 3D pose data are transmitted to the HMD device over the wireless network. A software application developed based on a unity engine [15] was installed on the HMD device. This software receives the relative 3D pose data over the wireless network and uses them to overlay the 3D spine model and needle path onto the back surface of the patient in real time. Real-time visualization is possible because the visual sensor of the HMD device can recognize the reference

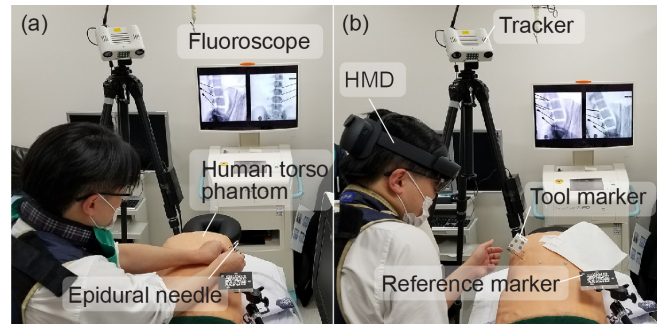


Fig. 5: Experimental setup: (a) Fluoroscopy-guided and (b) AR-assisted epidural needle interventions with a dynamic breathing phantom

marker coordinate system and trace its 3D pose in real time. The 3D pose of the marker attached to the epidural needle with respect to the reference marker coordinate system is also transmitted to the HMD device over the wireless network and used to visualize the 3D model of the epidural needle onto the HMD. The 3D model of the needle with the tool tracking marker was precisely constructed by measuring the actual tip position and direction of the needle using a caliper.

#### F. Experiment

An experiment was conducted to validate the feasibility of the proposed system. A human torso phantom, which includes vertebrae, spinal nerves, and intervertebral discs, was constructed based on real patient CT data, as shown in Fig. 5). Two human torso phantoms were prepared and used in the experiments. Prior to the experiment, CT data of the phantoms were obtained and used for the image-patient registration during the experimental procedure. For each phantom, a pain physician selected eight target points on the posterior-lateral edges of the discs located between L2 and sacrum using VR-based surgical planning software. Eight 14-gauge epidural needles were inserted into the targets. Four needles on the right side of the phantom were inserted based on the conventional fluoroscopy-guided approach, whereas four needles on the contralateral side of the phantom were inserted under the guidance of the proposed AR-assisted navigation system. The times required to insert a needle into the target and select an entry point on the back surface of the phantom were measured during the experiment. The number of X-ray images acquired for needle insertion was also counted during the experiment. A device capable of mimicking human respiration was developed and installed under the phantom to simulate patient movement arising from the respiration of the patient during the procedure. The same experimental procedure was repeated for the two phantoms.

To analyze the targeting accuracy, the phantoms were scanned using a CT device (Ingenuity Core 128, Philips, Netherlands) immediately after the experiment. The center points of the skin markers were then extracted from the volume data along with the epidural needle inserted into the phantom using the isosurface extraction algorithm [16]. The tip positions of the needle were manually selected from the



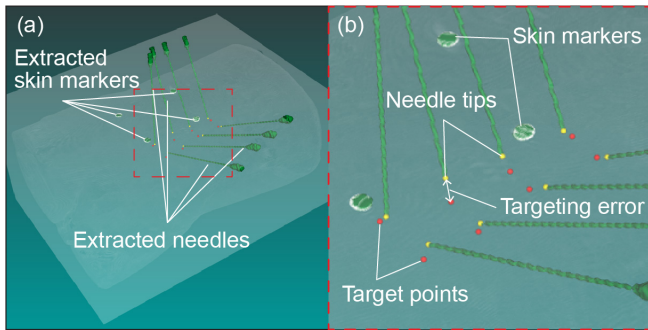


Fig. 6: Targeting error analysis, Trial1: (left) skin markers and needles extracted from CT volume, (right) targeting error defined as the distance between target point (red) and needle tip (yellow)

extracted needle models, as shown in Fig. 6). Eight target points determined by the pain physician were thereafter registered to the same coordinate system using the two sets of four center points of the skin markers extracted from the preoperative and postoperative CT volumes, respectively. The targeting error was calculated as the Euclidean distance between the needle tip and the corresponding target.

### III. RESULTS

Table I lists the time spent for the epidural needle insertion under the guidance of the fluoroscopic imaging system and the AR-assisted navigation system. The results demonstrate that the time required for the entry point selection was approximately five times shorter when using the AR-assisted navigation approach than when using the fluoroscopy-guided approach. The time required to insert the needle to the target point was approximately three times faster in the AR-assisted navigation approach compared to that of the conventional fluoroscopy-guided approach. Moreover, the number of X-rays required for the needle insertions was nearly three times less in the AR-assisted navigation approach than in the fluoroscopy-guided approach.

TABLE I: Time spent and number of X-rays required for fluoroscopy-guided vs. AR-guided epidural needle insertion

Criteria	Trial	Fluoroscopy-guided	AR-guided
Time Spent [sec]	Trial1	$58.6 \pm 44.3$	$11.1 \pm 12.3$
	Trial2	$190.4 \pm 49.1$	$76.1 \pm 28.8$
	Average	$124.5 \pm 46.7$	$43.6 \pm 20.6$
Number of X-rays	Trial1	$3.8 \pm 0.9$	$1.3 \pm 0.5$
	Trial2	$14.8 \pm 3.9$	$4.4 \pm 2.1$
	Average	$9.3 \pm 2.4$	$2.9 \pm 1.3$

TABLE II: Targeting errors

Trial Number	Target	Targeting Error [mm]	
		Fluoroscopy-guided	AR-guided
Trial1	T1(L2-L3)	7.16	5.20
	T2(L3-L4)	11.49	8.48
	T3(L4-L5)	6.57	12.14
	T4(L5-Sac.)	7.49	5.98
	Average	8.18	7.95
Trial2	T1(L2-L3)	5.78	4.40
	T2(L3-L4)	4.36	4.14
	T3(L4-L5)	6.56	6.95
	T4(L5-Sac.)	5.84	9.86
	Average	5.63	6.34

For all the needles, it was confirmed that the tip of the needle could be successfully placed at an acceptable targeting area for the phantom that mimics human lung respiration. Table II lists the targeting error for each needle insertion. The average needle targeting errors were  $6.91 \pm 2.09mm$  and  $7.14 \pm 2.82mm$  under the guidance of the fluoroscopic imaging system and the AR-assisted navigation system, respectively.

### IV. DISCUSSION AND CONCLUSION

We developed an AR-assisted surgical navigation system for epidural needle interventions. The experimental results demonstrated that the proposed approach enables intuitive and practical visual guidance for epidural needle insertion. The proposed system could also significantly reduce the time required for needle insertion and the number of X-rays required in the procedure under the guidance of the proposed method compared to the conventional approach. This may potentially decrease ionizing radiation exposure in patients and medical teams.

### REFERENCES

- [1] J. M. Mathis and S. Golovac, *Image-guided spine interventions*. Springer, 2011.
- [2] L. Al-Khouja, F. Shweikeh, R. Pashman, J. P. Johnson, T. T. Kim, and D. Drazin, "Economics of image guidance and navigation in spine surgery," *Surgical neurology international*, vol. 6, no. Suppl 10, p. S323, 2015.
- [3] T. Ungi, A. Lasso, and G. Fichtinger, "Tracked ultrasound in navigated spine interventions," in *Spinal Imaging and Image Analysis*. Springer, 2015, pp. 469–494.
- [4] N. C. Himes, T. Chansakul, and T. C. Lee, "Magnetic resonance imaging-guided spine interventions," *Magnetic Resonance Imaging Clinics*, vol. 23, no. 4, pp. 523–532, 2015.
- [5] J. D. Iannuccilli, E. A. Prince, and G. M. Soares, "Interventional spine procedures for management of chronic low back pain—a primer," in *Seminars in interventional radiology*, vol. 30, no. 3. Thieme Medical Publishers, 2013, p. 307.
- [6] A. Elmi-Terander, H. Skulason, M. Söderman, J. Racadio, R. Homan, D. Babic, N. van der Vaart, and R. Nachabe, "Surgical navigation technology based on augmented reality and integrated 3d intraoperative imaging: a spine cadaveric feasibility and accuracy study," *Spine*, vol. 41, no. 21, p. E1303, 2016.
- [7] T. M. Urakov, M. Y. Wang, and A. D. Levi, "Workflow caveats in augmented reality-assisted pedicle instrumentation: cadaver lab," *World neurosurgery*, vol. 126, pp. e1449–e1455, 2019.
- [8] P. Wei, Q. Yao, Y. Xu, H. Zhang, Y. Gu, and L. Wang, "Percutaneous kyphoplasty assisted with/without mixed reality technology in treatment of ovcf with ivc: a prospective study," *Journal of orthopaedic surgery and research*, vol. 14, no. 1, pp. 1–9, 2019.
- [9] W. J. Schroeder, B. Lorensen, and K. Martin, *The visualization toolkit: an object-oriented approach to 3D graphics*. Kitware, 2004.
- [10] L. Ibanez, W. Schroeder, L. Ng, and J. Cates, *The ITK software guide*. Kitware, 2003.
- [11] K. S. Arun, T. S. Huang, and S. D. Blostein, "Least-squares fitting of two 3-d point sets," *IEEE Transactions on pattern analysis and machine intelligence*, no. 5, pp. 698–700, 1987.
- [12] B. K. Horn, "Closed-form solution of absolute orientation using unit quaternions," *Josa a*, vol. 4, no. 4, pp. 629–642, 1987.
- [13] P. J. Besl and N. D. McKay, "Method for registration of 3-d shapes," in *Sensor fusion IV: control paradigms and data structures*, vol. 1611. International Society for Optics and Photonics, 1992, pp. 586–606.
- [14] J. Baek, G. Noh, and J. Seo, "Development and performance evaluation of wireless optical position tracking system," *J. Institute of Control, Robotics and Systems*, vol. 25, no. 12, pp. 1065–1070, 2019.
- [15] J. K. Haas, "A history of the unity game engine," 2014.
- [16] W. E. Lorensen and H. E. Cline, "Marching cubes: A high resolution 3d surface construction algorithm," *ACM siggraph computer graphics*, vol. 21, no. 4, pp. 163–169, 1987.